

1                   **Re-formulation of Plume Spread for Near-Surface Dispersion**

2                   Akula Venkatram<sup>1</sup>, Michelle G. Snyder<sup>2\*</sup>, David K. Heist<sup>2</sup>, Steven G. Perry<sup>2</sup>,

3                                   William B. Petersen<sup>3</sup>, Vlad Isakov<sup>2</sup>

4                                   <sup>1</sup>University of California, Riverside, CA 92521

5                   <sup>2</sup>U.S. Environmental Protection Agency, Office of Research and Development, National  
6                   Exposure Research Laboratory, Atmospheric Modeling and Analysis Division, Research  
7                                   Triangle Park, NC 27711 USA

8                                   <sup>3</sup>William B. Petersen, Consulting, Research Triangle Park, NC

9  
10  
11  
12  
13  
14  
15  
16  
17  
18  
19  
20  
21  
22  
23  
24  
25  
26  
27  
28  
29  
30  
31  
32  
33  
34  
35  
36                   \*corresponding author: Michelle G. Snyder (Snyder.Michelle@epa.gov).

## 37 **ABSTRACT**

38 Recent concerns about effects of automobile emissions on the health of people living close to  
39 roads have motivated an examination of models to estimate dispersion in the surface  
40 boundary layer. During the development of a new line source dispersion model, RLINE  
41 (Snyder et. al 2013), analysis of data from a tracer field study led to a re-examination of near-  
42 surface dispersion resulting in new formulations for horizontal and vertical plume spread  
43 presented in this paper. The equations for vertical spread use the solution of the two-  
44 dimensional diffusion equation, in which the eddy diffusivity, based on surface layer  
45 similarity, is a function of surface micrometeorological variables such as surface friction  
46 velocity and Monin-Obukhov length. The horizontal plume spread equations are based on  
47 Eckman's (1994) suggestion that plume spread is governed by horizontal turbulent velocity  
48 fluctuations and the vertical variation of the wind speed at mean plume height. Concentration  
49 estimates based on the proposed plume spread equations compare well with data from both  
50 the Prairie Grass experiment (Barad 1958) as well as the recently conducted Idaho Falls  
51 experiment (Finn et al. 2010). One of the major conclusions of this study is that the plume  
52 spreads as well as the wind speed used to estimate concentrations in a dispersion model form  
53 a set of coupled variables.

## 54 **KEYWORDS**

55 *Plume spread, near surface dispersion, surface releases, similarity theory, model*  
56 *performance, Prairie Grass experiment, Idaho Falls experiment, RLINE*

## 57 **1 Introduction**

58 New interest in modeling dispersion from surface releases has been sparked by recent studies  
59 showing that people living and working near roadways are exposed to elevated levels of  
60 pollution and are at increased risk of respiratory problems (e.g., Nitta et al. 1993; McConnell  
61 et al. 2006), birth and developmental defects (e.g., Wilhelm and Ritz 2003), premature  
62 mortality (e.g., Finkelstein et al. 2004; Jerrett et al. 2005), cardiovascular effects (e.g., Peters  
63 et al. 2004; Riediker et al. 2004), and cancer (e.g., Harrison et al. 1999; Pearson et al. 2000).  
64 The near roadway pollutants originate primarily from automobiles and trucks, which are near  
65 surface releases.

66 In response to this concern with the health effects, the USEPA initiated a program to examine  
67 the many factors that influence the dispersion of mobile source emissions and develop a line  
68 source model, RLINE (Snyder et. al. 2013), to model roadway impacts. The model  
69 development program included a tracer field study (Finn et al. 2010) in Idaho Falls to provide  
70 new data for examining near-surface dispersion from a line source. An analysis of the Idaho  
71 Falls data indicated that currently used dispersion curves (Briggs 1982; Venkatram 1992),  
72 based on the Prairie Grass field study (Barad 1958) do not provide a satisfactory description  
73 of both the new and historical data. This led to a reformulation of the plume spread  
74 equations, which is the primary topic of this paper.

## 75 **2 Current Plume Spread Formulation and Evaluation**

76 Vertical dispersion in the surface layer is well understood. The underlying theory has a long  
77 history (e.g. Chaudhry and Meroney 1973; Van Ulden 1978), and has been evaluated  
78 extensively with data from field studies and wind tunnel experiments. This theoretical  
79 understanding has been translated into formulations for plume spreads that are used in  
80 dispersion models such as AERMOD (Cimorelli et al. 2005). These formulations are

81 functions of micrometeorological variables, such as surface friction velocity and Monin-  
 82 Obukhov length, and have been evaluated with data from the Prairie Grass field study (Barad  
 83 1958). Examples are those proposed by Venkatram (1982) and Briggs (1982). A version of  
 84 this equation is included in AERMOD (Cimorelli et al. 2005).

85 The equations for plume spread are evaluated within the framework of the Gaussian  
 86 dispersion model for estimating the concentration at a receptor,  $(x,y,z)$ ,

$$\frac{C(x, y, z)}{Q} = \frac{1}{2\pi\sigma_z\sigma_y U} \left( \exp\left[-\frac{1}{2}\left(\frac{z-z_s}{\sigma_z}\right)^2\right] + \exp\left[-\frac{1}{2}\left(\frac{z+z_s}{\sigma_z}\right)^2\right] \right) \exp\left(-\frac{y^2}{2\sigma_y^2}\right), \quad (1)$$

87 where  $\sigma_y$  and  $\sigma_z$  are a measure of plume spread in the horizontal and vertical, respectively,  $Q$   
 88 is the emission rate,  $U$  is the near surface wind speed, and  $z_s$  is the source height.

89 In this paper, we adopt the plume spread equations incorporated in AERMOD (Cimorelli et  
 90 al. 2005; Venkatram 1992) to be representative of formulations in current use. The vertical  
 91 spread,  $\sigma_z$ , of a surface release is estimated from

$$\begin{aligned} \sigma_z &= \sqrt{\frac{2u_*x}{\pi U} \left(1 + 0.7\frac{x}{L}\right)^{-1/3}} \quad L > 0.0 \\ &= \sqrt{\frac{2u_*x}{\pi U} \left(1 + 0.0006\left(\frac{x}{L}\right)^2\right)^{1/2}} \quad L < 0.0 \end{aligned} \quad (2)$$

92 where  $L$  is the Monin-Obukhov length defined by  $L = -T_0 u_*^3 / (\kappa g Q_0)$ ,  $Q_0$  is the surface  
 93 kinematic heat flux,  $u_*$  is the surface friction velocity,  $g$  is the acceleration due to gravity,  $T_0$  is  
 94 a reference temperature, and  $\kappa$  is the von Karman constant taken to be 0.40.

95 The horizontal spread of the plume used in Equation (1) is a purely empirical equation that  
 96 fits the data from Prairie Grass (Cimorelli et al. 2005):

$$\begin{aligned} \sigma_y &= \frac{\sigma_v x}{U} (1 + 78X)^{-0.33} \\ \text{where } X &= \frac{\sigma_v x}{U z_i} \end{aligned} \quad (3)$$

97 and  $\sigma_v$  is the standard deviation of the horizontal velocity fluctuations and  $z_i$  is the mixed  
 98 layer height.

99 Under low wind speeds, horizontal meandering of the wind spreads the plume over large  
 100 azimuth angles, which might lead to concentrations upwind relative to the vector averaged  
 101 wind direction. We account for meandering by adopting the approach in AERMOD  
 102 (Cimorelli et al. 2005) which assumes that when the mean wind speed is close to zero, the  
 103 horizontal plume spread covers 360°. Then, the concentration is taken to be a weighted  
 104 average of concentrations of two possible states: a random spread state, and a plume state. In  
 105 the random spread state, the release is allowed to spread radially in all horizontal directions.  
 106 Then, the horizontal distribution in Equation (1) is replaced by:

$$H(x, y, r) = f_r \frac{1}{2\pi r} + (1 - f_r) \frac{1}{\sqrt{2\pi}\sigma_y} \exp\left(-\frac{y^2}{2\sigma_y^2}\right), \quad (4)$$

107 where the first term represents the random state in which the plume spread covers  $2\pi$  radians,  
 108 and  $r$  is the distance between the source and receptor. The second term is the plume state  
 109 corresponding to the Gaussian distribution.

110 The plume is transported at an effective velocity given by

$$U_e = (\sigma_x^2 + \sigma_y^2 + U(\bar{z})^2)^{1/2} = (2\sigma_y^2 + U(\bar{z})^2)^{1/2}, \quad (5)$$

111 where  $U(\bar{z})$  is the wind speed evaluated at the mean plume height and the expression assumes  
 112 that  $\sigma_y \approx \sigma_x$ . The mean plume height,  $\bar{z}$ , a function of vertical spread, is formulated in section  
 113 3. Note that the effective velocity is non-zero even when the mean velocity is zero. The  
 114 minimum value of the effective velocity,  $U_e$ , is  $\sqrt{2}\sigma_y$ .

115 The weight for the random component in Equation (4) is taken to be

$$f_r = \frac{2\sigma_y^2}{U_e^2}. \quad (6)$$

116 This ensures that the weight for the random component goes to unity when the mean wind  
 117 approaches zero. The success of this meandering correction depends on measurements of  $\sigma_y$ ,  
 118 which presumably reflect meandering when the wind speed is close to zero. If measurements  
 119 are not available, we have to estimate  $\sigma_y$  from other meteorological variables (see Cimorelli  
 120 et al. 2005).

121 The need to specify an effective wind speed,  $U_e$ , in Equations (1) thru (6) highlights a problem  
 122 with the application of the Gaussian dispersion equation to releases in the surface layer, where  
 123 the wind speed varies rapidly with height. However, if the source height and the receptor  
 124 height are close to zero, and the receptor is close to the line source, the ground-level  
 125 concentration is insensitive to the choice of the height to evaluate the wind speed because the  
 126 ground-level concentration is inversely proportional to the product  $\sigma_z U$  (see Equation 2), which

127 is independent of  $U$ . When the release and receptor heights are non-zero, the concentration  
128 becomes more sensitive to  $U$ . This point is discussed in detail in section 3.

129 We first examine the performance of current formulations for plume spread using data from  
130 the two field studies described next.

## 131 2.1 Evaluation with Prairie Grass Field Study

132 In each experiment of the Prairie Grass Project (Barad 1958) the tracer,  $\text{SO}_2$ , was released from  
133 a point location at a height of 0.46 m, for an interval of 10 min, and the concentration was  
134 sampled along five semi-circular arcs at distances of 50, 100, 200, 400, and 800 m from the  
135 release. The samplers on the arcs were spaced at  $2^\circ$  intervals on the first four arcs, and at  $1^\circ$  on  
136 the 800-m arc for a total of 545 sampler locations. Roughly half of the 70 experiments were  
137 conducted under stable conditions, which covered both low and high wind-speed conditions.  
138 The mean wind was measured at 8 levels ranging from 0.125 m to 16 m. The standard  
139 deviation of the horizontal wind direction and vertical velocity fluctuations used in this study  
140 were derived from bivane measurements at a height of 2 m. The micrometeorological inputs,  
141  $u_g$  and  $L$ , computed by fitting M-O velocity and temperature profiles to tower measurements,  
142 are taken from van Ulden (1978). Lee and Irwin (1997) fitted Gaussian distributions to the  
143 concentrations along each arc and derived horizontal spreads and peak concentrations for each  
144 arc. These data were obtained from Aarhus University, Denmark at  
145 <http://envs.au.dk/en/knowledge/air/models/background/omlprairie/excelprairie/>.

146 Model performance estimates of concentration are compared qualitatively to measurements  
147 with the use of scatter plots. In addition, model performance is quantified using the  
148 performance statistics as described in Venkatram (2008). The quantitative model  
149 performance measures used here are the geometric mean bias ( $m_g$ ), the geometric standard  
150 deviation ( $s_g$ ) and the fraction of estimates within a factor of two of the measured value  
151 (fac2). Venkatram's definition of  $m_g$  suggests that a model is over predictive when  $m_g < 1$ .  
152 We have flipped the ratio of observed-to-predicted concentrations here, so that  $m_g > 1$  is  
153 indicative of a model over-prediction;  $m_g < 1$  is indicative of a model under-prediction. To  
154 avoid the effect of outliers on the computation of these statistics, we use the following  
155 definitions of the geometric mean bias and standard deviation:

156

$$m_g = \text{median} \left( \frac{C_p}{C_o} \right) \quad (7)$$

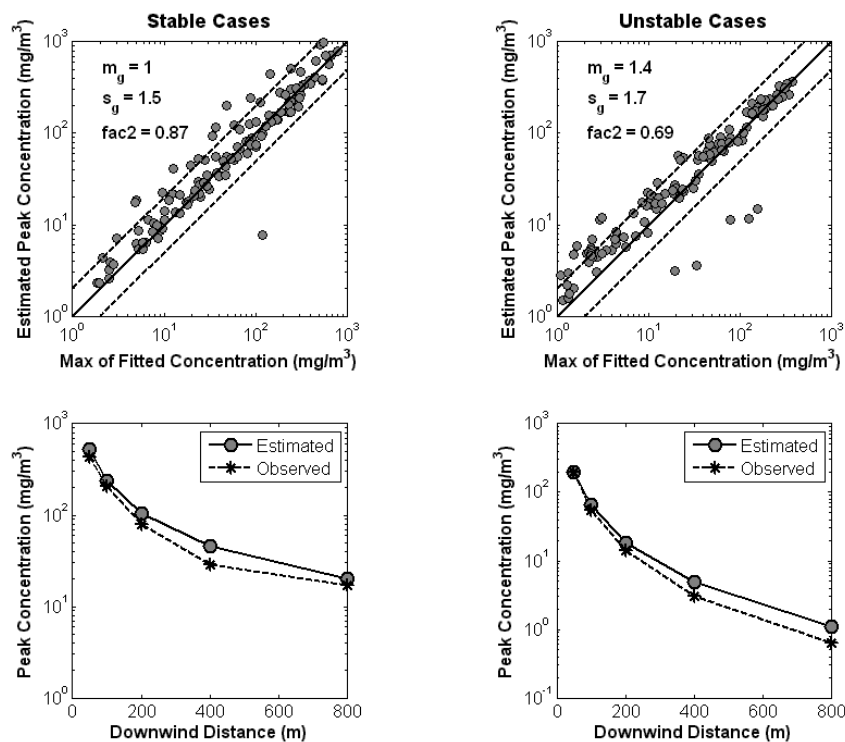
157 and

$$s_g = \exp \left( \frac{\ln(F)}{\sqrt{2} \operatorname{erf}^{-1}(A_F)} \right), \quad (8)$$

158 where  $C$  is the concentration, either observed (subscript 'o') or predicted (subscript 'p'),  $F$  is  
159 taken to be 2,  $A_F$  is the fraction of the ratio,  $C_p/(C_o m_g)$ , between  $1/F$  and  $F$ , and  $\operatorname{erf}^{-1}$  is

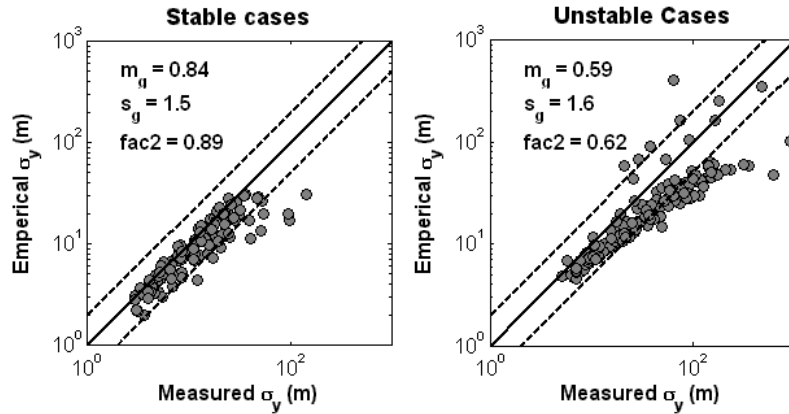
160 the inverse error function. Equation (26) is equivalent to fitting a lognormal distribution to  
 161 the values of  $C_p/C_o$  between 0.5 and 2, so  $s_g$  equals one when 100% of the predictions lie  
 162 within a factor of two interval. Only when values are outside of a factor of two interval is the  
 163 value of  $s_g$  greater than one. Observed and predicted concentrations are paired in time and  
 164 space.

165 Figure 1 shows the performance of Equations (2) and (3) applied within the RLINE  
 166 framework, a line source model described in the companion paper (Snyder et al. 2013). While  
 167 this model is based on numerically approximating a line with point sources, in this  
 168 application we used the calculation of concentration from one point source. The model is  
 169 generally unbiased in stable conditions and overestimates in unstable conditions. Although  
 170 there is inevitable scatter, most of the model estimates are within a factor of two of the  
 171 observations. The bottom panel of Figure 1 shows that the model has a tendency to  
 172 overpredict the peak concentrations at all downwind distances for all conditions.



173  
 174 **Figure 1: Comparison of concentration estimates from Equations (1-6) to observations at**  
 175 **Prairie Grass. Bottom panel compares mean of the estimated peak concentrations at each**  
 176 **downwind distance with corresponding observations.**

177 The performance of Equation (3) in describing the horizontal spread is seen in Figure 2. The  
 178 observed horizontal spreads were estimated by fitting a Gaussian distribution to the ground-  
 179 level concentration at each radial distance from the source. The biases in  $\sigma_y$  contribute to the  
 180 biases seen in the estimated concentrations presented in Figure 1.



181

182 **Figure 2: Comparison of  $\sigma_y$  estimates from Equations (3) with measured values at Prairie**  
 183 **Grass. The solid line represents the one-to-one line, the parallel dashed lines represent**  
 184 **factor of two intervals.**

185 How do these dispersion formulations derived from Prairie Grass work for Idaho Falls? We  
 186 briefly describe the Idaho Falls experiment before answering this question.

187 **2.2 Evaluation with Idaho Falls Field Experiment**

188 The field study was conducted in 2008 (Finn et al. 2010) near NOAA’s Grid 3 diffusion grid  
 189 at the Department of Energy’s Idaho National Laboratory (INL). The Grid 3 area on the INL  
 190 is located across a broad, relatively flat plain on the western edge of the Snake River Plain in  
 191 southeast Idaho. The objective of the study was to examine the impact of roadway sound  
 192 barriers on dispersion of emissions from a line source. The tracer, SF<sub>6</sub>, was released  
 193 simultaneously from two 54m line sources positioned one meter above ground level,  
 194 representing pollutant source roadway. One of the releases was 6 m upwind (generally) of a  
 195 90 meter long and 6 meter high noise barrier while the other release was without a barrier.  
 196 The tracer was sampled on identical grids of 58 samplers extending out to 180 m in the  
 197 general downwind direction from the source. Two of the samplers were deployed upwind of  
 198 the release line to check for possible upwind tracer dispersion. Bag samplers were positioned  
 199 at 1.5 m AGL in a rectangular array from 18 to 180 meters downwind of the source line. The  
 200 SF<sub>6</sub> tracer was simultaneously released from the line source for each grid beginning 15 min  
 201 before the sampler measurements started to establish a quasi-steady state concentration field  
 202 and continued until the end of each test. An array of six 3-d sonic anemometers was  
 203 deployed for sensing winds and turbulence. Five tests were conducted during the study, each  
 204 spanning a 3-h period broken into 15-min tracer sampling intervals. One test was conducted  
 205 in unstable conditions, one in neutral conditions, and three in stable conditions. The  
 206 micrometeorological conditions corresponding to these test are shown in Table 1.

207 **Table 1: Summary of the conditions during each day of the Idaho Falls 2008 field test.**

Test Day	L (m)	$u_*$ (m/s)	Reference Wind Speed (m/s)	Wind Direction (deg)
1 – Slightly Convective	-(500-181.8)	0.52-0.88	5.5-8.1	192.7-228.1
2 - Convective	-(29.8-1.7)	0.15-0.34	0.7-2.5	189-203.9
3 – Slightly Stable	+(35.3-62.0)	0.28-0.35	3.2-3.6	202-208.6

5 - Stable	+(4.9-17.3)	0.05-0.19	1.6-2.4	194.1-230.8
------------	-------------	-----------	---------	-------------

208

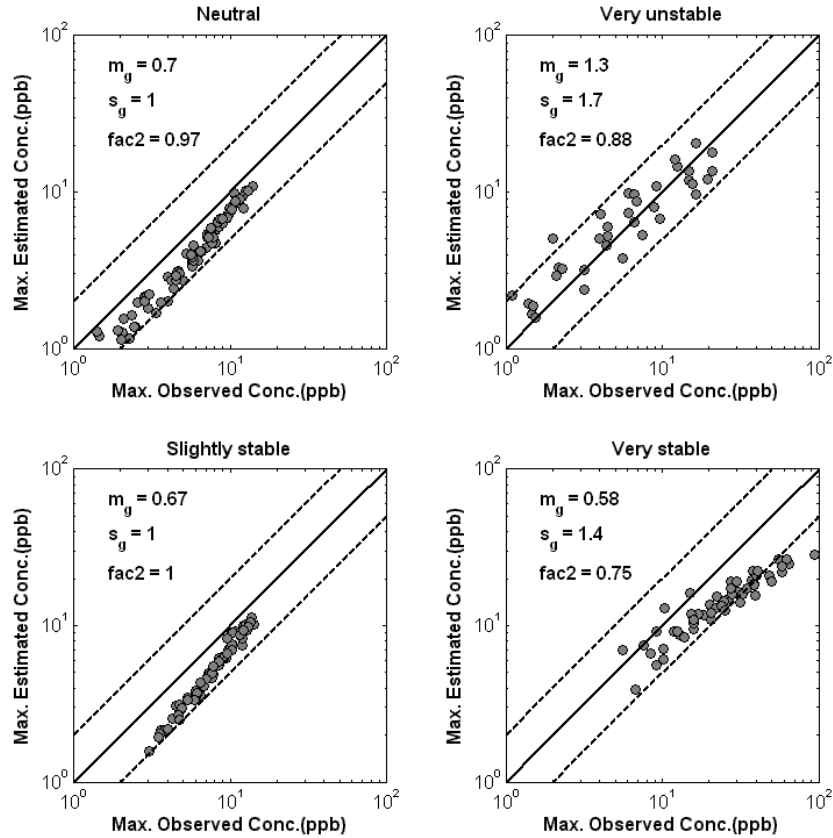
209 The sampler density was greatest near the sources and decreased in the downwind direction.  
 210 A single tracer line source was used to simulate roadway emissions for the primary and  
 211 control experimental grids.

212 Test 1 was conducted on October 9, 2008 from 1230-1530 hours Mountain Standard Time  
 213 (MST) in neutral stability conditions. Winds were generally well in excess of  $5 \text{ m s}^{-1}$  and  
 214 skies were heavily overcast. Test 2 was conducted on October 17, 2008 from 1300-1600  
 215 hours MST in unstable conditions. Skies were clear and sunny throughout the test period and  
 216 winds were light from 1 to 3 m/s. Test 3 was conducted on October 18, 2008 from 1600-  
 217 1900 hours MST in weakly stable conditions. The wind direction was very close to ideal  
 218 until the last hour of the experiment when a transition in the wind field occurred. Skies were  
 219 clear throughout the experiment. Test 4 was conducted in moderately to strongly stable  
 220 conditions but was not used because the wind direction was unfavourable with respect to the  
 221 source and sampler grid orientation. Test 5 was conducted on October 24, 2008 from 1800-  
 222 2100 hours MST in moderate to strongly stable conditions.

223 Again we computed the concentrations associated with the finite line source using RLINE  
 224 (Snyder et al. 2013) with the dispersion parameters of Equations (2) and (3). The surface  
 225 roughness length,  $z_0$ , was found to be 0.053 m, which was obtained by fitting the Monin-  
 226 Obukhov (MO) similarity profile to the wind speeds measured at the 3 m sonic anemometer  
 227 level during a set of trials in which the wind direction was within 20 degrees from the normal to  
 228 the line source.

229 Figure 3 shows the comparison between concentration estimates and concentrations made at the  
 230 samplers in the Idaho Falls experiments. The model estimates and the observations correspond  
 231 to the maximum at each downwind distance. Although there is a high degree of correlation  
 232 between model estimates and observations, the concentrations are underestimated at low  
 233 concentrations for the neutral and slightly stable cases. There is a slight tendency for the  
 234 concentrations to be overestimated during the highly unstable conditions of Test 2. During the  
 235 very stable conditions of Test 5, there are a number of concentration values that are  
 236 underestimated by close to a factor of two.

237 Although most of the model estimates are within a factor of two of the observed values, it is  
 238 clear from Figure 3 that the discrepancies show a trend with concentrations. The  
 239 concentrations during stable and neutral conditions are substantially underestimated. These  
 240 results motivated a reexamination of the plume dispersion equations, which we describe in the  
 241 next section.



242

243 **Figure 3: Comparison of maximum concentration estimates based on plume dispersion**  
 244 **equations (1) to (3) with corresponding observations from Idaho Falls. The solid line**  
 245 **represents the one-to-one line, the parallel dashed lines represent factor of two intervals.**

246 **3 Reformulated Plume Spreads and Evaluation**

247 The starting point of the reformulation is the model proposed by van Ulden (1978) and  
 248 evaluated with observations from the Prairie Grass experiment (Barad 1958). This model,  
 249 which is similar to those developed by others (Chaudry and Meroney 1973), is based on the  
 250 solution of the eddy diffusivity based mass conservation equation. This starting point,  
 251 together with the observation that mean plume height and vertical spread are closely related  
 252 parameters, suggests beginning with a derivation of the mean plume height and then relating  
 253 that to vertical spread.

254 The crosswind integrated concentration associated with a point source at ground-level with  
 255 strength  $Q$ , is taken to satisfy

$$U(z) \frac{\partial C}{\partial x} = \frac{\partial}{\partial z} \left( K(z) \frac{\partial C}{\partial z} \right) \tag{9}$$

256 If we assume that the wind speed,  $U(z)$ , and the eddy diffusivity  $K(z)$  are described by  
 257 power laws

$$U(z) = U_r \left( \frac{z}{z_r} \right)^p \tag{10}$$

258 and

$$K(z) = K_r \left( \frac{z}{z_r} \right)^n \quad (11)$$

259 where  $U_r$  and  $K_r$  are values at a reference height  $z_r$ , Equation (9) has the solution

$$\frac{C(x, z)}{Q} = \frac{A}{\bar{U} \bar{z}} \exp \left[ - \left( \frac{Bz}{\bar{z}} \right)^s \right] \quad (12)$$

260 where the mean plume velocity,  $\bar{U}$ , and mean plume height,  $\bar{z}$ , are defined by

$$\bar{U} = \frac{\int C U(z) dz}{\int C dz} \quad \text{and} \quad \bar{z} = \frac{\int C z dz}{\int C dz}, \quad (13)$$

261 the constants in the solution are

$$B = \frac{\Gamma(2/s)}{\Gamma(1/s)} \quad \text{and} \quad A = \frac{sB}{\Gamma(1/s)}, \quad (14)$$

262 where  $\Gamma(p)$  is the gamma function given by  $\int_0^\infty x^{p-1} \exp(-x) dx$ , and

$$s = p - n + 2. \quad (15)$$

263 From the relationship for plume variance (i.e.  $\sigma_z^2 = \int z^2 C dz / \int C dz$ ) the mean plume  
264 height,  $\bar{z}$ , is related to plume spread by

$$\sigma_z = f_z \bar{z}, \quad (16)$$

265 where  $f_z = \left( \frac{\Gamma(3/s) \Gamma(1/s)}{\Gamma(1/s) B^2} \right)^{1/2}$ . Substituting Equations (10) and (12) into Equation (13) results in

$$\bar{U} = f_u U_r \left( \frac{\bar{z}}{z_r} \right)^p = f_u U(\bar{z}), \quad (17)$$

$$\text{where } f_u = \Gamma \left( \frac{p+1}{s} \right) / \left[ \Gamma \left( \frac{1}{s} \right) B^p \right].$$

266 The important result that is used in the subsequent analysis can be derived from the previous  
267 equations (van Ulden 1978):

$$\frac{d\bar{z}}{dx} = s B^s \frac{K(\bar{z})}{U(\bar{z}) \bar{z}}. \quad (18)$$

268 Because  $\bar{z}$  is related to the plume  $\sigma_z$  through Equation (16), the result (18) becomes the  
269 primary equation to estimate plume spread. As in van Ulden (1978), we will assume that  
270 Equation (18) holds even when Equation (15) is not satisfied. The justification is provided by  
271 the results obtained by van Ulden (1978).

272 To make progress, we will assume that at the asymptotic limits of neutral, stable, and  
273 unstable conditions, the eddy diffusivity can be written as  $K(z) = \alpha u_* z^n |L|^{1-n}$ , where  $\alpha$  is a

274 constant. Note  $n=1$  represents neutral conditions,  $n=0$  to very stable conditions, and  $n=3/2$  to  
 275 very unstable conditions.

276 Then, if we substitute Equations (10) and (11) into Equation (18) and integrate, we find

$$\bar{z} \sim \left[ \frac{u_s}{U_s} x |L|^{1-n} z_s^n \right]^{\frac{1}{(n+2-n)}}, \quad (19)$$

277 which reduces, using Equation (10), to

$$\bar{z} \sim \left[ \frac{u_s}{U(\bar{z})} x |L|^{1-n} \right]^{\frac{1}{(2-n)}}. \quad (20)$$

278 Note that Equation (20) is implicit in  $\bar{z}$  because  $U$  is evaluated at  $\bar{z}$ . We compute the wind  
 279 speed at the mean plume height by solving the following equation iteratively,

$$\sigma_z = f(x, u_s, L, U(\bar{z})), \quad (21)$$

280 where the mean plume height for a Gaussian distribution is given by

$$\bar{z} = \sigma_z \sqrt{\frac{2}{\pi}} \exp \left[ -\frac{1}{2} \left( \frac{z_s}{\sigma_z} \right)^2 \right] + z_s \operatorname{erf} \left( \frac{z_s}{\sqrt{2} \sigma_z} \right). \quad (22)$$

281 From Equation (22) the mean plume height depends on the vertical spread.

### 282 3.1 Vertical Spread, $\sigma_z$

283 To obtain an expression for  $\sigma_z$  for neutral conditions ( $n=1$ ), we use the relationship between  
 284  $\sigma_z$  and  $\bar{z}$  (from Equation (16)) to reduce Equation (20) to:

$$\sigma_z = a \frac{u_s x}{U_s}, \quad (23)$$

285 where  $a$  is a constant that is evaluated empirically. In applications of this model,  $U_s$  is  
 286 substituted for  $U(\bar{z})$ , see Equation (5).

287 The stable velocity asymptote  $U(\bar{z}) \sim u_s \bar{z} / L$  leads to  $\sigma_z \sim L^{2/3} x^{1/3}$  and an equation that  
 288 interpolates between the neutral and stable limits becomes

$$\sigma_z = a \frac{u_s}{U_s} x \frac{1}{\left( 1 + b_s \frac{u_s}{U_s} \left( \frac{x}{|L|} \right)^{2/3} \right)}. \quad (24)$$

289 To derive the unstable  $\sigma_z$  asymptote, we take  $n=3/2$ , and obtain

$$\sigma_z \sim (u_s/U_s)^2 x^2 / |L|, \quad (25)$$

290 and the semi-empirical formulation for  $\sigma_z$  under unstable conditions becomes

$$\sigma_z = u \frac{u_s}{U_s} x \left( 1 + k_u \left( \frac{u_s x}{U_s |L|} \right) \right). \quad (26)$$

291 Note that these expressions for  $\sigma_z$  are implicit because the wind speed,  $U_s$ , on the right hand  
 292 side of the equation is a function of  $\bar{z}$ , which in turn is a function of  $\sigma_z$ .

293 Briggs (1982) and Venkatram (1982; 1992) used a similar approach to connect the asymptotic  
 294 limits of the crosswind integrated concentrations. But they used the expression for the  
 295 crosswind concentration to derive the expression for the vertical plume spread rather than  
 296 connecting the asymptotes of the actual plume spreads, as we have done here. This explains  
 297 the difference between the current formulation and the earlier ones.

### 298 3.2 Horizontal Spread, $\sigma_y$

299 Estimates of horizontal dispersion in the surface layer are largely based on Taylor's theory  
 300 (1921) for dispersion in homogeneous turbulence based on a Lagrangian time scale, i.e. travel  
 301 time. However, travel time cannot be defined unambiguously because the wind speed varies  
 302 with height, therefore there is no theoretically justified choice for the Lagrangian time scale.

303 Equations currently in use for  $\sigma_y$ , such as those proposed by Irwin (1983) and Draxler (1976),  
 304 use the wind speed at a specific height, usually the source height, to estimate the travel time  
 305 and the Lagrangian time scale is a purely empirical fit. Eckman (1994) showed that the  
 306 variation of  $\sigma_y$  with distance, the initial linear increase followed by a smaller increase with  
 307 distance (or travel time) could be explained by the increase of the wind speed with height if  
 308 one assumed that  $\sigma_y$  is governed by the small time expression

$$\frac{d\sigma_y}{dx} = \frac{\sigma_y}{\bar{U}}, \quad (27)$$

309 where  $\sigma_y$  is the standard deviation of the horizontal velocity fluctuations, even when it does  
 310 not vary with height, and the mean plume velocity,  $\bar{U}$ , is defined by the Equation (13).

311 Using a numerical solution of Van Ulden's (1978) expression for  $\bar{z}$ , Eckman (1994) showed  
 312 that Equation (27) provides an excellent description of horizontal spread data from a variety of  
 313 studies. Thus, Eckman's formulation avoids the arbitrariness entailed in specifying travel time  
 314 and it also incorporates our current understanding of the effects of stability on dispersion.  
 315 Eckman (1994) provides a useful analytical approximation for  $\sigma_y$  based on the numerical  
 316 integration of Equation (27). In this paper, we adopt Equation (27) to derive expressions for the  
 317 horizontal spread,  $\sigma_y$ . We integrate Equation (27) using Equations (17) and (20) to obtain

$$\sigma_y \sim \frac{\sigma_z}{u_*} \sigma_z \left( \frac{\sigma_z}{|L|} \right)^{1-n} \quad (28)$$

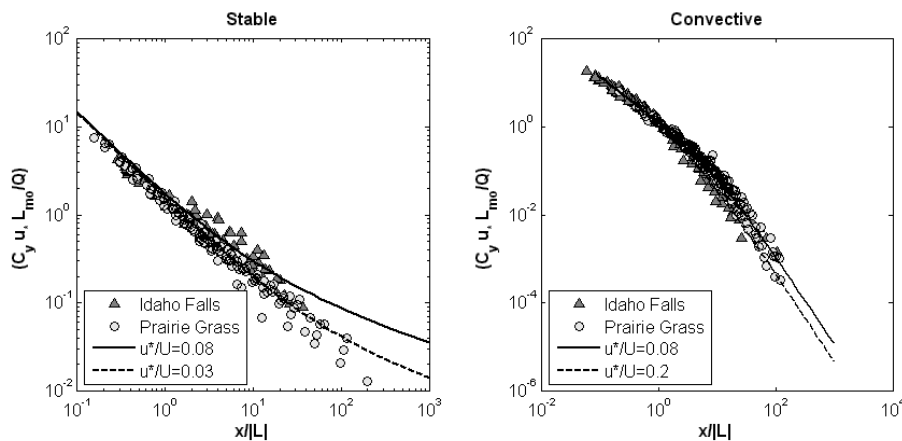
318 taking  $\bar{z}$  as a constant fraction of  $\sigma_z$ . An expression for  $\sigma_y$  that interpolates between the  
 319 neutral and very stable and unstable conditions is given by

$$\sigma_y = c \frac{\sigma_z}{u_*} \sigma_z \left( 1 + d \frac{\sigma_z}{|L|} \right)^{1-n} \quad (29)$$

320 where  $c$  and  $d$  are empirical constants; the value of  $d$  depends on the sign of  $L$ . Note that the  
 321 wind speed and the vertical and horizontal spreads that appear in the equation to compute  
 322 concentration depend on each other, and cannot be calculated independently.

### 323 3.3 Evaluation of plume spread equations with Prairie Grass and Idaho Falls data

324 We can evaluate the empirical constants in the vertical spread equations, (24) and (26), at  
 325 Prairie Grass and Idaho Falls by comparing the measured and modeled crosswind integrated  
 326 concentrations. The measurements from a finite line source (54 meters) at Idaho Falls were  
 327 converted to those corresponding to an equivalent infinite line source using an approach  
 328 described in (Heist et al. 2009).  $C_y$ , the crosswind integrated concentrations, is inversely  
 329 proportional to  $\sigma_z$  when scaled with  $u^*$ ,  $L$  and  $Q$ . Since  $\sigma_z$  is a strong function of  $x/|L|$  and a  
 330 weaker function of  $u^*/U_*$ , Figure 4 shows a comparison of the normalized concentration ( $C_y$ )  
 331 as a function of  $x/|L|$  for values of  $u^*/U_*$  that are representative of the range of observations  
 332 in the two field studies. Based on this analysis the coefficients from Eqn. (24) and (26) that  
 333 best represent these data sets are  $a = 0.57$ ,  $b_s = 1.5$  and  $b_u = 0.5$ .

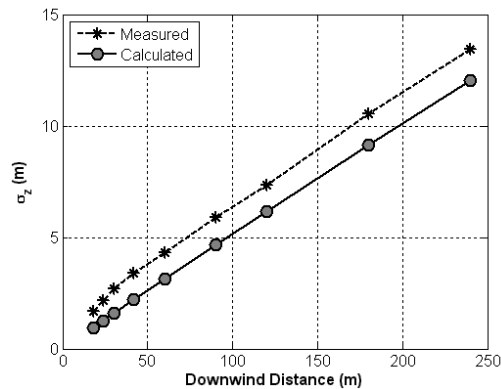


334  
 335 **Figure 4: Idaho Falls 2009 (▲) and Prairie Grass (○) normalized concentration vs.**  
 336  **$x/|L|$ . The solid and dashed lines represent Equation (24), for stable, and Equation (26),**  
 337 **for convective, with  $u^*/U_*$  values representative of the range of values in the field**  
 338 **studies.**

339 We further test this new vertical dispersion formulation by using measured  $\sigma_z$  from the wind  
 340 tunnel studies. A series of wind tunnel experiments were performed in EPA boundary-layer  
 341 wind tunnel (Heist et al. 2009) to examine the effect of roadway configurations (including  
 342 noise barriers and roadway depression relative to the surrounding terrain) on the dispersion of  
 343 traffic-related pollutants. The data for a flat roadway are used here in evaluating the vertical

344 dispersion formulations. Vertical concentration fields (typically unavailable in field studies)  
345 are particularly useful for estimating vertical dispersion.

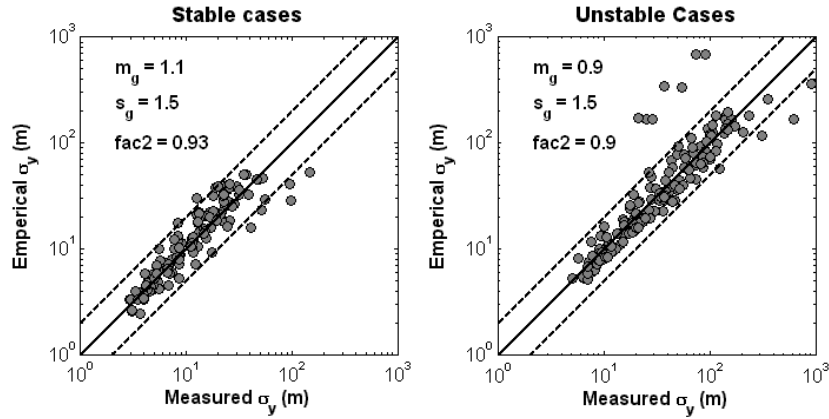
346 In Figure 5 the measured  $\sigma_z$  values from the wind tunnel experiment are shown with the  
347 calculated  $\sigma_z$  using Equation (26) at the neutral limit. We assume that the emissions are at a  
348 height of 0.9 m with  $\sigma_{z0} = 0.4$  m. (based on the size of the roughness elements on the model  
349 roadway). The apparent offset between the modeled and measure  $\sigma_z$  is likely to be from the  
350 initial mixing near the source. However, this figure shows agreement between the measured  
351 and calculated vertical dispersion growth rates.



352  
353 **Figure 5: Calculated and measured wind tunnel  $\sigma_z$  as a function of downwind distance.**  
354 **The  $\sigma_z$  was calculated with a source height of 0.9 m and an initial  $\sigma_z$  of 0.4 m.**

355 For the horizontal dispersion formulation (29), we used the Prairie Grass data to determine  
356 the coefficients. The  $\sigma_y$ 's were determined by fitting a Gaussian distribution to the  
357 concentrations measured at each downwind distance. Based on the comparison of Equation  
358 (29) for  $\sigma_y$  with these estimates, the coefficients that best represent these data were found to  
359 be  $a = 1.6$  (for all conditions) and  $d = 2.5$  for stable conditions and  $d = 1$  for convective  
360 conditions.

361 The comparisons of model to data using these coefficients are shown in Figure 6. Overall,  
362 these new horizontal dispersion formulations produce geometric mean values near unity for  
363 all stabilities and nearly all of the estimated  $\sigma_y$  values are within a factor of two of the  
364 observed values. In addition, comparison of Figures 2 and 6 shows that the new horizontal  
365 spread equations describe the data considerably better than the empirical Equation (3).



366

367 **Figure 6: Comparison of  $\sigma_y$  estimates from new equations (30b and 31b) with measured**  
 368 **values from the Prairie Grass field study.**

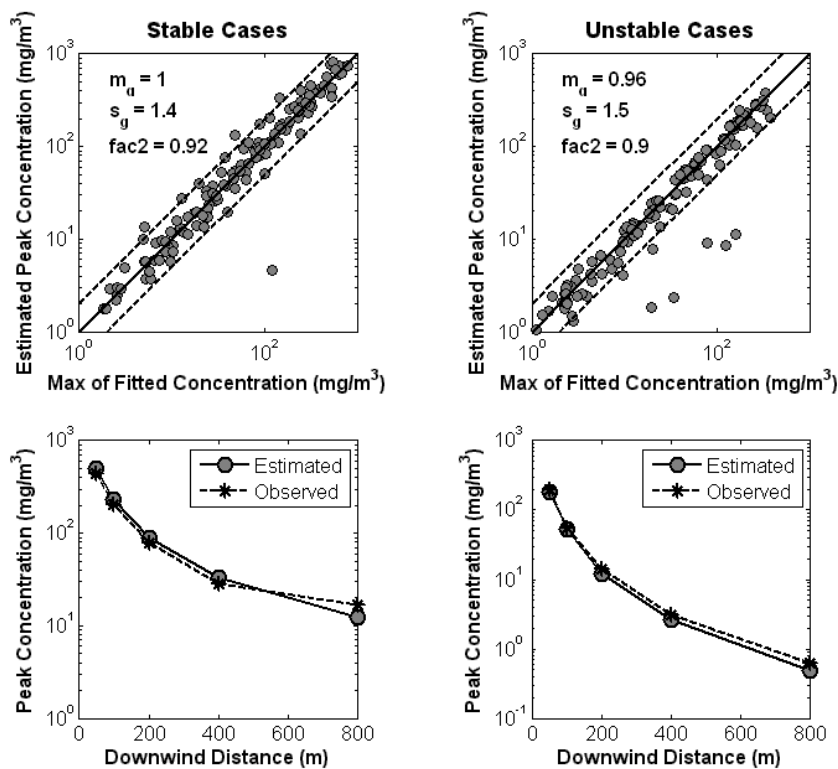
369 The constants that provide the best fit between model estimates for the vertical spread are:

$$\begin{aligned} \sigma_z &= 0.57 \frac{u_x}{U_x} x \left( 1 + 3 \frac{u_x}{U_x} \left( \frac{x}{L} \right)^{2/3} \right)^{-1} \text{ for } L > 0.0 \\ &= 0.57 \frac{u_x}{U_x} x \left( 1 + 1.5 \left( \frac{u_x x}{U_x |L|} \right) \right) \text{ for } L < 0.0 ; \end{aligned} \quad (30)$$

370 and for the horizontal spread are:

$$\begin{aligned} \sigma_y &= 1.6 \frac{\sigma_v}{u_x} \sigma_z \left( 1 + 2.5 \frac{\sigma_z}{L} \right) \text{ for } L > 0.0 \\ &= 1.6 \frac{\sigma_v}{u_x} \sigma_z \left( 1 + \frac{\sigma_z}{|L|} \right)^{-1/2} \text{ for } L < 0.0. \end{aligned} \quad (31)$$

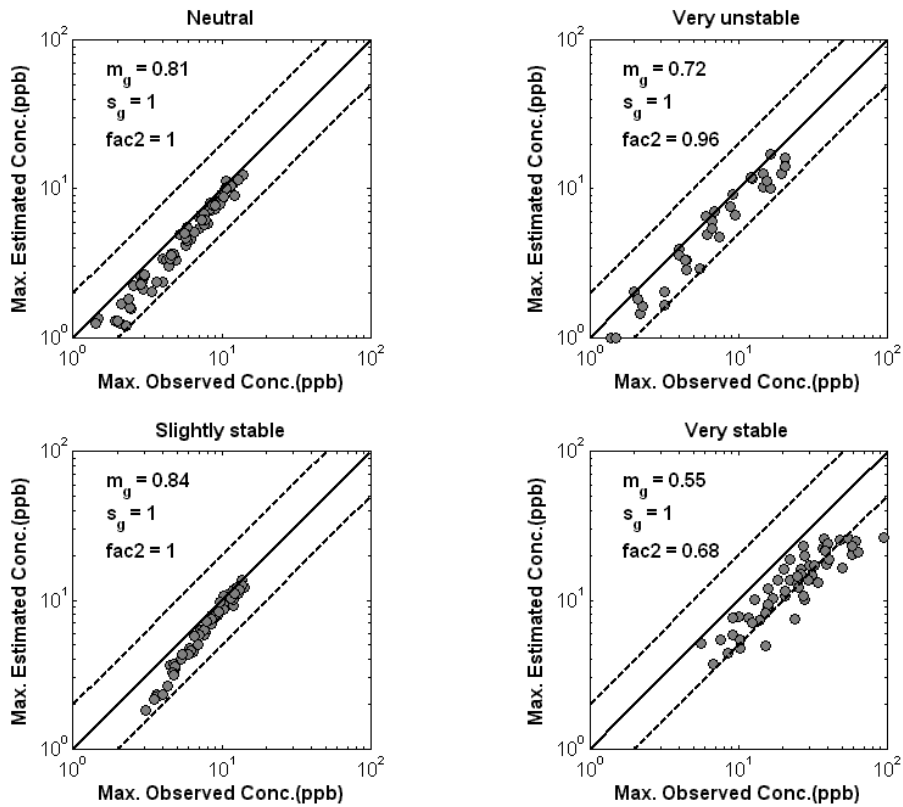
371 A comparison of Figures 1 and 7 shows the new formulations for plume spreads yield  
 372 concentration estimates that compare better with observed values (at Prairie Grass) than those  
 373 based on the earlier equations (2) and (3).



374

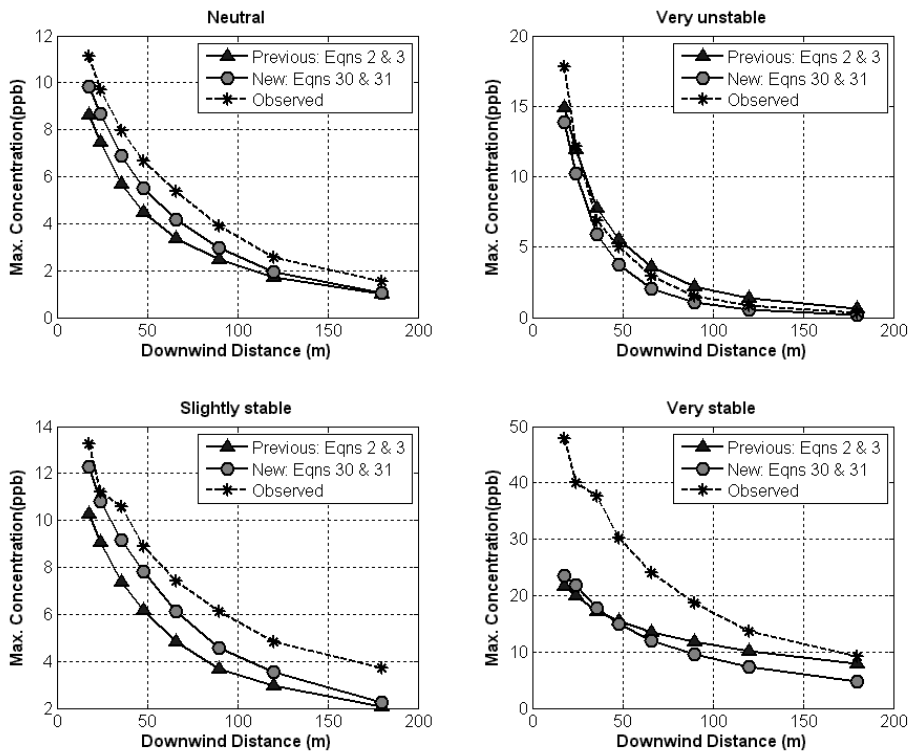
375 **Figure 7: Comparison of concentration estimates from new equations (30) and (31) to**  
 376 **observations at Prairie Grass. Bottom panel compares mean of the maximum estimated**  
 377 **concentrations at each downwind distance with corresponding observations.**

378 As Figure 3 indicates for Idaho Falls, Equations (2) and (3) applied within the RLINE model  
 379 yield concentration estimates that show systematic biases relative to the observed values.  
 380 These biases are reduced substantially in the results corresponding to Equations (30) and (31)  
 381 as seen by comparing Figure 3 and 7. Looking at the concentration profile as a function of  
 382 downwind distance (Figure 9) the new formulations, provide improvement. However,  
 383 concentrations are still underestimated particularly for the very stable cases. This  
 384 underestimation is substantially reduced if RLINE is run without the meander algorithm,  
 385 which suggests that the treatment of wind meander might require modification.



386

387 **Figure 8: Comparison of maximum concentration estimates based on new dispersion**  
 388 **equations (30) and (31) with corresponding observations from Idaho Falls. Parallel lines**  
 389 **denote factor of two intervals.**



390

391 **Figure 9: Comparison of mean maximum modeled concentrations at each downwind**  
 392 **distance with corresponding observations at Idaho Falls.**

#### 393 **4 Summary**

394 Results from a recently conducted field study in Idaho Falls (Finn et al. 2010) allowed us to  
395 re-examine dispersion formulations for near-surface releases. This paper proposes new  
396 formulations for horizontal and vertical plume spread for releases in the near surface  
397 boundary layer. The equations for vertical spread are functions of downwind distance and  
398 surface micrometeorological variables including surface friction velocity and Monin-  
399 Obukhov length. The theoretical foundation of these equations is the mass conservation  
400 equation expressed in terms of the eddy diffusivity based on surface layer similarity. This  
401 approach has been demonstrated by Van Ulden (1978) and others (Gryning et al. 1983) to  
402 provide an excellent description of dispersion of surface releases.

403 The horizontal plume spread equations are based on Eckman's (1994) suggestion that  
404 horizontal plume spread is governed by horizontal turbulent velocity fluctuations and the  
405 vertical variation of the wind speed at mean plume height. The resulting equations explicitly  
406 relate horizontal plume spread to vertical plume spread, and do not contain any references to  
407 a Lagrangian time scale, which is often used in currently used formulations (Irwin, 1983 for  
408 example). The new equations for horizontal plume spread yield estimates that compare well  
409 with observations from the Prairie Grass experiment.

410 Concentration estimates based on the proposed plume spread equations compare well with  
411 data from the Prairie Grass experiment (Barad 1958) as well as the recently conducted Idaho  
412 Falls experiment (Finn et al. 2010). One of the major conclusions of this study is that the  
413 plume spreads as well as the wind speed used to estimate concentrations are variables that  
414 need to be consistent with each other.

#### 415 **5 Acknowledgements**

416 The authors would like to thank our colleagues Drs. Kirk Clawsen, Denis Finn, and Richard  
417 Eckman of the National Oceanic and Administration's Air Resources Laboratory for  
418 providing the Idaho Falls tracer data and for their insightful interpretation of the data.

419 The authors would also like to thank the members of the U. S. EPA near-road program. The  
420 authors are grateful to Dr. Valerie Garcia of EPA's National Exposure Research Laboratory,  
421 and Dr. Richard Baldauf of the EPA Office of Transportation and Air Quality for their  
422 collaboration throughout the model development process. In addition, we are thankful for the  
423 laboratory support from Dr. Laurie Brixey.

#### 424 **6 Disclaimer**

425 The United States Environmental Protection Agency through its Office of Research and  
426 Development funded and managed the research described here. It has been subjected to  
427 Agency's administrative review and approved for publication.

#### 428 **7 REFERENCES**

- 429 Barad, M., 1958. Project Prairie Grass. A field program in diffusion AF-CRF-TR-58-235.
- 430 Brauer, M., Hoek, G., Van Vliet, P., Meliefste, K., Fishcer, P.H., Wijga, A.; Koopman, L.P.,  
431 Neijens, H.J., Gerritsen, J., Kerkhof M., Heinrich J., Bellander, T., Brunekreef, B., 2002.  
432 Air Pollution from Traffic and the Development of Respiratory Infections and Asthmatic

- 433 and Allergic Symptoms in Children. *American Journal of Respiratory and Critical Care*  
434 *Medicine*, **166**, 1092-1098.
- 435 Briggs, G. A. 1982. Similarity forms for ground-source surface-layer diffusion. *Boundary*  
436 *Layer Meteorology*, **23**, 489-502.
- 437 Chaudhry, F.H., Meroney, R.H., 1973. Similarity Theory of Diffusion and the Observed  
438 Vertical Spread in the Diabatic Surface Layer. *Boundary Layer Meteorology*, **3**, 405-415.
- 439 Cimorelli, A.J., S.G. Perry, A. Venkatram, J.C. Weil, R.J. Paine, R.B. Wilson, R.F. Lee,  
440 W.D. Peters, R.W. Brode, 2005. AERMOD: A Dispersion Model for Industrial Source  
441 Applications. Part I: General Model Formulation and Boundary Layer Characterization.  
442 *Journal of Applied Meteorology*, **44**, 682-693.
- 443 Draxler, R.R. 1976. Determination of atmospheric diffusion parameters. *Atmospheric*  
444 *Environment.*, **10**, 99-105.
- 445 Eckman, R.M. 1994. Re-examination of empirically derived formulas for horizontal diffusion  
446 from surface sources. *Atmospheric Environment.*, **28**, 265-272.
- 447 Finkelstein, M.M., Jerrett, M., Sears, M.R., 2004. Traffic Air Pollution and Mortality Rate  
448 Advancement Periods. *American Journal of Epidemiology.*, **160**, 173-177.
- 449 Finn, D., Clawson, K.L., Carter, R.G., Rich, J.D., Eckman, R.M., Perry, S.G., Isakov, V.,  
450 Heist, D.K., 2010. Tracer studies to characterize the effects of roadside noise barriers on  
451 near-road pollutant dispersion under varying atmospheric stability conditions.  
452 *Atmospheric Environment*, **44**, 204-214.
- 453 Gryning S.E., van Ulden A.P., Larsen S., 1983. Dispersion from a Ground Level Source  
454 Investigated by a K-Model, Quarterly Journal of the Royal Meteorological Society 109,  
455 355-364.
- 456 Harrison, R.M., Leung, P.L., Somerville, L., 1999. Analysis of incidence of childhood  
457 cancer in the West Midlands of the United Kingdom in relation to the proximity of main  
458 roads and petrol stations. *Journal of Occupational and Environmental Medicine*, **56**, 774-  
459 780.
- 460 Hoek, G., Brunekreef, B., Goldbohm, S., Fischer, P., van den Brandt, P.A., 2002. Association  
461 Between Mortality and Indicators of Traffic-related Air Pollution in the Netherlands: a  
462 Cohort Study. *Lancet*, **360**, 1203-1209.
- 463 Irwin, J. S., 1983. Estimating plume dispersion: a comparison of several sigma schemes.  
464 *Journal of Applied Meteorology*, **22**, 92-114.
- 465 Jerrett, M., Burnett, R. T., Pope III, C.A., Krewski, D., Newbold, K.B., Thurston, G., Shi, Y.,  
466 Finkelstein, N., Calle, E.E., Thun, M.J., 2005. Spatial analysis of air pollution and  
467 mortality in Los Angeles. *Epidemiology*, **16**, 727-736.
- 468 Kim, J.J., Smorodinsky, S., Ostro, B., Lipsett, M., Singer, B.C., Hogdson, A.T., 2002.  
469 Traffic-related Air Pollution and Respiratory Health: the East Bay Children's Respiratory  
470 Health Study. *Epidemiology*, **13**, S100.
- 471 McConnell, R., Berhane, K., Yao, L., Jerrett, M., Lurmann, F., Gilliland, F., Kuenzli, N.,  
472 Gauderman, J., Avol, E., Thomas, D., Peters, J., 2006. Traffic, susceptibility, and  
473 childhood asthma. *Environmental Health Perspectives*, **114**, 766-772.
- 474 Nitta, H., Sato, T., Nakai, S., Maeda, K., Aoki, S. and Ono, M., 1993. Respiratory health  
475 exposure associated with exposure to automobile exhaust. I. Results of cross-sectional  
476 studies in 1979, 1982, and 1983. *Archives of Environmental Health*, **48**, 53-58.

- 477 Pearson, R.L., Wachtel, H., Ebi, L., 2000. Distance-weighted traffic density in proximity to a  
478 home is a risk factor for leukemia and other childhood cancers. *Journal of the Air and*  
479 *Waste Management Association*, **50**, 175-180.
- 480 Peters, A., von Klot, S., Heier, M., Trentinaglia, I., Hormann, A., Wichmann, E., Lowel, H.,  
481 2004. Exposure to traffic and the onset of myocardial infarction. *New England Journal*  
482 *of Medicine*, **351**, 1721-1730.
- 483 Riediker, M., Cascio, W.F., Griggs, T.R., Herbst, M.C., Bromber, P.A., Neas, L., Williams,  
484 R., Devlin, R.B., 2004. Particulate matter exposure in cars is associated with  
485 cardiovascular effects in healthy, young men. *American Journal of Respiratory and*  
486 *Critical Care Medicine*, **169**, 934-940.
- 487 Snyder, M.G., Venkatram, A., Heist, D.K., Perry, S.G., Petersen, W.B., Isakov, V., 2013:  
488 RLINE: A Line Source Dispersion Model for Near-Surface Releases. *Atmospheric*  
489 *Environment (submitted)*.
- 490 van Ulden, A.P., 1978. Simple estimates from vertical dispersion from sources near the  
491 ground. *Atmospheric Environment*, **12**, 2125-2129.
- 492 Venkatram, A. 1982. A semi-empirical method to compute concentrations associated with  
493 surface releases in the stable boundary layer. *Atmospheric Environment*, **16**, 245-248.
- 494 Venkatram, A. 1992. Vertical dispersion of ground-level releases in the surface boundary  
495 layer. *Atmospheric Environment*, **26A**, p947-949.
- 496 Venkatram, A., and T.W. Horst, 2006. Approximating dispersion from a finite line source.  
497 *Atmospheric Environment*, **40**, 2401-2408.
- 498 Venkatram, A., 2008. Computing and Displaying Model Performance Statistics. *Atmospheric*  
499 *Environment*, **42**, 6882-6868.
- 500 Wilhelm, M., B. Ritz, February, 2003. Residential Proximity to Traffic and Adverse Birth  
501 Outcomes in Los Angeles County, California, 1994-1996. *Environmental Health*  
502 *Perspectives*, **111**, 207-216.